ISSN 1066-3622, Radiochemistry, 2021, Vol. 63, No. 6, pp. 843–850. © Pleiades Publishing, Inc., 2021.
Russian Text © The Author(s), 2021, published in Radiokhimiya, 2021, Vol. 63, No. 6, pp. 582–590.

Immobilization of Technetium into a Sodium-Aluminum-Iron Phosphate Glass: Degree of Oxidation of Technetium and Iron, Hydrothermal Stability of the Glass

S. S. Danilov[a,*], A. V. Frolova[a], A. Yu. Teterin[b], K. I. Maslakov[c], Yu. A. Teterin[a,b], S. A. Kulikova[a], and S. E. Vinokurov[a]

[a] *Vernadsky Institute of Geochemistry and Analytical Chemistry, Russian Academy of Sciences, Moscow, 119334 Russia*
[b] *Kurchatov Institute Scientific Research Center, Moscow, 123098 Russia*
[c] *Lomonosov Moscow State University, Moscow, 119991 Russia*
** e-mail: danilov070992@gmail.com*

Received October 5, 2020; revised June 1, 2021; accepted June 8, 2021

Abstract—Glass samples containing 3 wt % of $KTcO_4$ have been synthesized in the system, mol %: $40Na_2O$–$10Al_2O_3$–$10Fe_2O$–$40P_2O_5$. The glass samples have been studied by X-ray photoelectron spectroscopy. It was found that the degree of technetium oxidation is Tc(IV), which differs from the behavior of rhenium under similar conditions: about 83% of Fe is present as Fe(III), and the rest, as Fe(II). A high stability of the lass against leaching at 90°C was demonstrated in the half-dynamic test (State Standard R 52126–2003): the rate of Tc leaching from the glass is about 3×10^{-6} g/(cm^2 day).

Keywords: immobilization, vitrification, aluminum-iron phosphate glass, technetium, X-ray photoelectron spectroscopy

DOI: 10.1134/S1066362221060175

INTRODUCTION

The ecologically safest way to handle high-activity wastes (HAWs) is to include these into solid highly stable matrices placed in storages. At present, the only industrially implemented technology for immobilization of HAWs is their vitrification with aluminum-phosphate or boron-silicate glass.

The ^{99}Tc radionuclide is a fission product contained in a spent nuclear fuel (SNF); the yield in fission in thermal reactors is 6.1 wt %, the annual amount of ^{99}Tc generated in a light-water reactor with power of 1000 MW is 21 kg [1]. The half-decay time of ^{90}Tc is 213 thousand years. Under the environmental conditions, Tc in the form of a pertechnetate ion is highly mobile, which presents a high radioecological hazard. Its high-temperature immobilization is complicated by the volatility of most of its compound. According to [2], more than 90% of ^{99}Tc is volatilized in the course of synthesis of a boron-silicate glass at 1150–1250°C.

We have developed previously the composition of sodium-aluminum-iron phosphate (SAIP) glass with high crystallization and hydrolytic stability, mol %: $40Na_2O$–$10Al_2O_3$–$10Fe_2O$–$40P_2O_5$ [3–8]. The synthesis temperature of the SAIP glass is about 900–1000°C, whuch must diminish the loss of Ts in its immobilization. We have shown previously that, in synthesis of a glass with Re as an imitator of ^{99}Tc, about 70% of Re introduced at similar synthesis temperatures (950°C) is immobilized.

Re is frequently used as an imitator of the ^{99}Tc isotope as an element with a similar chemical behavior. Nevertheless, the standard reduction potentials of Tc and Re at degrees of oxidation from (VII) to (IV) at 25°C are different; 0.74 and 0.51 V, respectively [10]. In a borosilicate glass in the presence of iron oxides, rhenium is in the states Re(VII) and Re(0), in contrast to technetium, which is mostly in the oxidation state (IV) [11]. Thus, Re may be an insufficiently correct imitator of ^{99}Tc under redox conditions.

The goal of the present study was to determine the oxidation states of technetium and iron in a SAIP glass and find the hydrothermal stability of the glass against leaching to assess the possibility of using the SAIP glass as a matrix for immobilization of 99Tc.

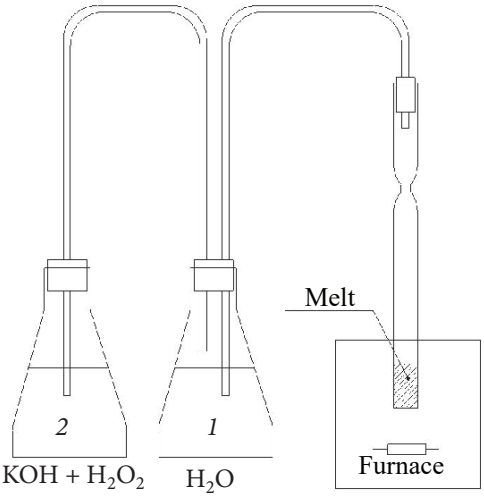

Fig. 1. Closed system for synthesis of a technetium-containing glass. (*1*) Flask with water and (*2*) flask with KOH and H_2O_2.

EXPERIMENTAL

The SAIP glasses were synthesized by melting the stock at 950°C in a high-temperature laboratory resistance furnace. The mixture was composed of $NaPO_3$, Al_2O_3, and Fe_2O_3 powders taken in amounts corresponding to the above-specified optimal composition of the SAIP glass, to which was added 3 wt% of $KTcO_4$ having higher melting (532°C) and decomposition (~1000°C) points as compared with $NaTcO_4$ [13]. SAIP glasses with technetium (in what follows designated as Tc-SAIP glasses) were synthesized in a closed volume to preclude the carryover of technetium (Fig. 1). An analysis of solutions 1 and 2 demonstrated that technetium is present in amounts of up to 30 wt % relative to the introduced amount of ^{99}Tc, including washouts from the surfaces of the tube and connecting elements. Previously, it has been shown [14] in a study by powder X-ray diffractometry and scanning electron microscopy of samples of the SAIP glass containing rhenium in an amount similar to the amount of technetium in our samples of Tc-SAIP that the resulting glass is X-ray-amorphous and homogeneous with a uniform volume distribution of all the components. Thus, it is expected that the state of the SAIP glass is similar when ^{99}Tc is added in the same amounts.

The surface elemental composition of the glass and the degree of oxidation of its constituent elements were examined by X-ray photoelectron spectroscopy (XPS) on a Kratos Axis Ultra DLD spectrometer with AlK_a monochromatic radiation (hν = 1486.7 eV) at an X-ray tube power of 150 W and pressure of 1.3×10^{-7} Pa at room temperature. The binding energies (E_b) were measured relative to the E_b of C1*s*-electrons of hydrocarbons adsorbed on the sample surface, taken to be 285.0 eV. The line halfwidths (Γ, eV) are presented relative to the linewidth of C1*s*-electrons of hydrocarbons on the sample surface, taken to be 1.3 eV [4]. The spectra were recorded with special software and a discharging device that stabilized the constant charging of a sample. First, each spectrum from the electron binding energies in the range from 0 to 1250 eV was scanned successively once and then the procedure was repeated the necessary times at a stable charging of a sample. The error in determining the binding energy and widths of the peaks did not exceed ±0.05 eV and that for the relative peak intensity, ±5%. The background associated with inelastically scattered electrons was subtracted by the Shirley method [15].

A sample of the Tc-SAIP glass for XPS measurements was produced as a cleavage of a bulk piece of the glass, which was pressed into indium on a steel plate (10 × 10 × 0.4 mm^3) and then attached to a holder with a double-side nonconducting adhesive band. A quantitative elemental analysis of the sample surface (thickness of the layer being analyzed was ~5 nm [16]), based on the fact that the intensity of XPS lines is proportional to the concentration of ions in a sample under study, was performed with the use of the relation $n_i/n_j = (S_i/S_j)(k_j/k_i)$, where n_i/n_j is the relative concentration of the atoms under study, S_i/S_j is the relative intensity (area) of the lines of electrons from the inner shells of these atoms, and k_j/k_i is the experimental relative-sensitivity coefficient. The following values were used for the sensitivity coefficients with respect to carbon: 1.00 (C1*s*), 2.805 (O1*s*), 0.69 (Al2p), 1.75 (P2*p*), 5.27 (K2*p*), 6.06 (Na1*s*), 10.64 (Fe2*p*).

Because the sensitivity coefficient for Tc cannot be found in the literature, its concentration n_{Tc} relative to the concentration of phosphorus atoms, n_P, on the sample surface was estimated by formula (1):

$$n_{Tc}/n_P = [(I_{Tc}\sigma_P)/(I_P\sigma_{Tc})][(\hbar\omega - E_{bP})/(\hbar\omega - E_{bTc})]^{1/2}, \quad (1)$$

where I_{Tc}/σ_P and I_P/σ_{Tc} are products of the intensity of technetium (phosphorus) line by the cross-section of photoionization of the corresponding subshell of phosphorus (technetium) [17], $\hbar\omega$ is the energy of the exciting *X* radiation, and E_{bP} (E_{bTc}) is the binding energy of phosphorus (technetium) electrons.

The hydrolytic stability of the Tc-SAIP glass was found by the method specified by State Standard R

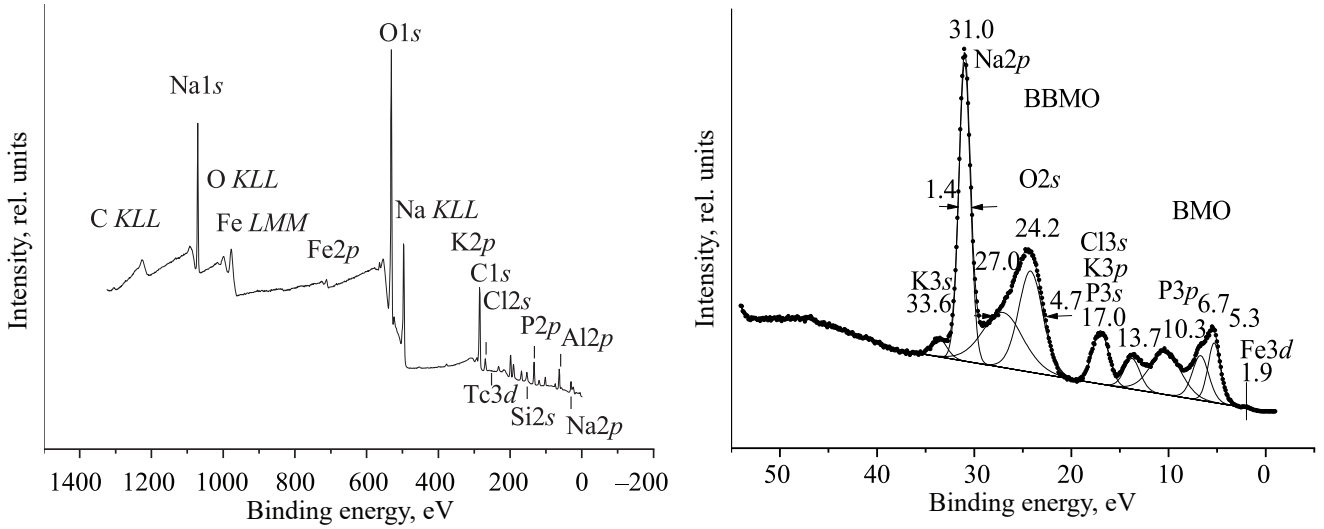

Fig. 2. (a) Panoramic XPS spectrum and (b) spectrum of valence electrons of the synthesized Tc–SAIP glass.

52126–2003 at 90 ± 2°C in the course of 28 days. The test used monolithic glass samples, with the contacting solution (twice-distilled water) replaced 1, 3, 7, 10, 14, 21, and 28 days after the beginning of a run. The content of technetium in the solutions after leaching was determined by the method of liquid scintillation spectrometry (Tri-Carb 2810 TR, Perkin-Elmer).

The leaching rates of the elements were calculated by formula (2):

$$LR_i = \frac{m_{ni}}{M_{0,i} S \Delta t}, \quad (2)$$

where m_{ni} is the mass of an element, leached out during nth period, g; $M_{0,i}$ is mass concentration of the element in a sample at the beginning of tests, g/g; S, area of the sample surface, cm^2; Δt is the leaching duration, days.

The leaching mechanism of Na and Tc from the glass was estimated in accordance with the de Groot and van der Sloot's model [18], which can be represented as Eq. (3) describing a linear dependence:

$$\log Y_i = A \log t + const, \quad (3)$$

where Y_i is the total output of element i from a sample during its contact with water, mg/m^2; and t is the contact duration, days.

RESULTS AND DISCUSSION

The panoramic XPS spectrum of the Tc-SAIP glass (Fig. 2a) shows lines of glass elements, saturated hydrocarbons, and Auger spectra of carbon (C *KLL*), oxygen (O *KLL*), iron (Fe *LMM*), and sodium (Na i). The energy range of this spectrum can be divided in two parts: low-energy range of spectrum of mostly valence electrons (0 to ~50 eV) and the part of core electrons with binding energies of ~50 eV and higher.

Structure of the spectra of valence electrons. The low-energy part of the spectrum of the Tc-SAIP glass show lines associated with electrons from the outer valence molecular orbitals (VMOs) at 0 to ~15 eV and inner valence molecular orbitals (IVMOs) at ~15 to ~50 eV (Fig. 2b, Table 1). The highest intensity peaks are observed at binding energies of O2*s*- and Na2*p*-electrons.

The spectrum of VMO electrons contains a number of characteristic peaks, but this gives no way of obtaining a quantitative information about the ionic composition of a sample. As noted in [19], the appearance of a low-intensity peak at 1.9 eV is supposedly due to the formation of a minor amount of $NaFePO_4$, which contains Fe^{2+} ions ($3d^6$).

It was also found in [19] that the states of O2*p*-electrons mostly form the outer valence band having a width of 10.4 eV. It was shown that a noticeable contribution to the spectrum of VMO electrons is made by the states of P3*s*-electrons at 13.3, 17.0, and 24.2 eV, and the states of P3*p*-electrons contribute to the peak at 10.3 eV (Fig. 2b). Because of being involved in the chemical bonding, the line of O2*s*-electrons is strongly broadened (Γ(O2*s*) = 4.2 eV) as compared with the line of O1*s*-electrons (Γ(O1*s*) = 2.1 eV) constituted by several components. A line whose intensity is contributed by P3*s*-, K3*p*-, and C13*s*-electrons is observed at 17.0 eV. A high-intensity line of Na2*p*-electrons is observed to be comparatively narrow [Γ(Na2*p*) = 1.4 eV]. Its width

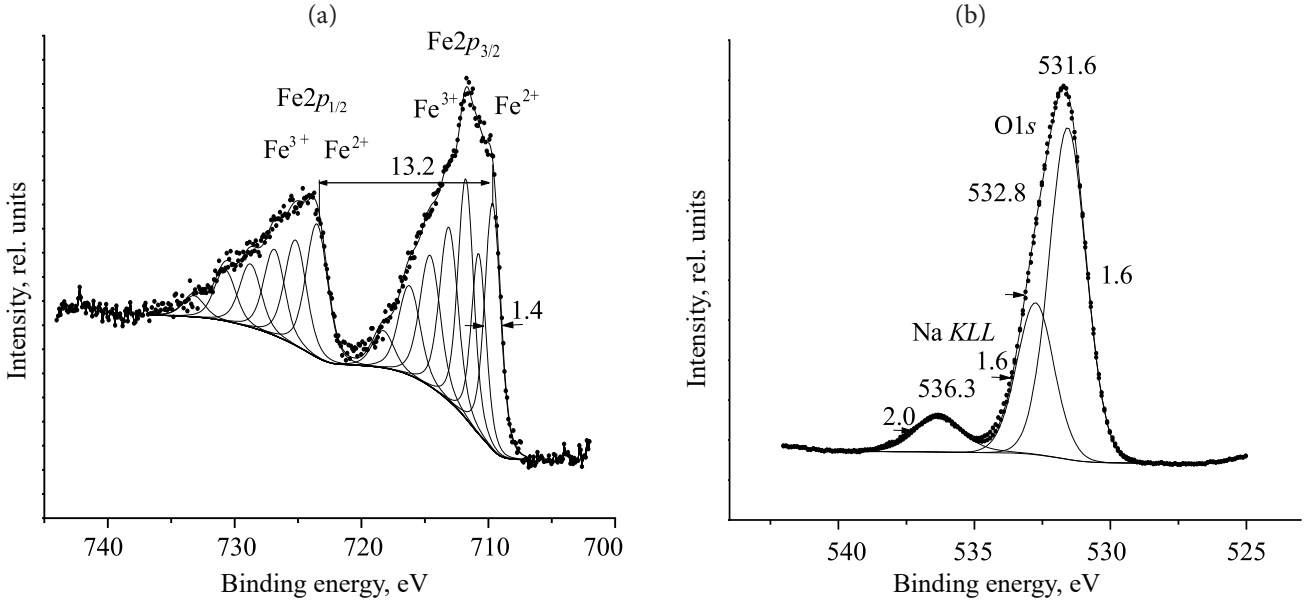

Fig. 3. XPS spectra of (a) Fe2p- and (b) O1s-electrons.

is comparable with the corresponding value for the line of Na1s-electrons [Γ(Na1s) = 1.5 eV]. The line of K3s-electrons is observed at 33.6 eV. The spectrum of valence electrons qualitatively reflects the elemental composition of the surface of the glass under study.

Structure of the spectra of core electrons. The quantitative stoichiometric and ionic composition of a glass can be determined on the basis of intensities, binding energies, and structure of the lines of core electrons of the constituent elements: Al2p-, P2p-, Tc3d-, Fe2p-, Na1s- K2p-, and O1s-electrons (Table 1). It is noteworthy that the binding energies of Al2p-electrons for the glass under study and Al_2O_3 [20] differ only slightly. The binding energy of Na1s-electrons in the glass under study is 0.7 eV lower than that for Na_2O. The zero shift of the line of Al2p-electrons is presumably due to the weak change in the structure of the nearest environment of aluminum atoms in the course of glass formation. The decrease in the binding energy of Na1s-electrons, associated with the increase in the charge on an atom, may be due to the decrease in the length of the ionic bond Na–O.

The XPS spectrum of Fe2p-electrons has a complex structure (Fig. 3a). As noted previously in [19], these spectra show a superposition of the spectra of Fe^{2+} and Fe^{3+} ions. It is supposed that the Fe^{2+} ($3d^6$) ions are in the small-spin (S = 0) Fe^{2+} ($t_{2g}^6e_g^0$) state and their spectrum is constituted by a doublet with relatively narrow lines with ΔE_{sl} = 13.2 eV. The components of this doublet are observed in the total spectrum as shoulders on the side with a lower binding energy from the main lines at (E_b(Fe2$p_{3/2}$) = 709.7 eV with Γ(Fe2$p_{3/2}$) = 1.5 eV. Only the maxima of these components are designated in Fig. 3a. Ions Fe^{3+}($3d^5$) are in a high-spin (S = 5/2) state Fe^{2+}($t_{2g}^3e_g^2$). A complex structure associated with the multiplet splitting appears in the spectrum of ions of this kind [21]. Therefore, there appears a doublet with broadened components (Γ(Fe2$p_{3/2}$) ≈ 5 eV), average value ΔE_{sl} = 13.2 eV, and characteristic shake-up satellites [22]. The ionic composition of iron in the Tc-SAIP is 83% Fe^{3+} and 17% Fe^{2+}. This agrees with the data on the retention of Tc, reported in 11]: at this Fe^{2+}/Fe_{tot} ratio, 50% of Tc was retained in the glass, with Tc^{4+}/Tc_{tot} being 50.

The spectrum of P2p-electrons is constituted by a single relatively narrow line (Table 1). This agrees with the data of [19, 23] and confirms that the glass contains stable PO_4^{3-} tetrahedra.

The line of O1s-electrons in the sample under study is broadened and asymmetric. This is due to the presence on the sample surface of oxygen ions in various chemical states (Fig. 3b). A Na KLL line of the Auger spectrum of sodium is observed near the line of O1s-electrons. The spectrum of O1s-electrons was resolved into two lines (Fig. 3b; Table 1), as this commonly done for spectra of glasses on silicate and phosphate bases. The binding energy of 531.6 eV is related to nonbridging ions, and 532.8 eV, to bridging oxygen ions, mostly to P–O–P bonds in the presence of a certain contribution from P–O–Al and

Table 1. Binding energies E_b(eV) of electrons and linewidths Γ (eV, in parentheses) for a Tc-SAIP sample

Sample	Valence band	Tc3$d_{5/2}$	Al2p	P2p	Fe2$p_{3/2}$	Na1s	K2$p_{3/2}$	O1s	C1s
Tc-SAIP	1.9, 5.3, 6.7, 10.3, 13.7, 17.0, 24.2, 27.1, 31.0, 33.6	257.6 (1.7), ΔE_{sl} = 3.6	75.0 (1.5), ΔE_{sl} = 0.4	133.9 (1.8), ΔE_{sl} = 1.0	709.7 Fe^{2+} (1.4), 710.8 Fe^{3+}, ΔE_{sl} = 13.1	1071.8 (1.5)	293.3 (1.6), ΔE_{sl} = 2.9	531.6 (1.6), 532.8 (1.6)	285.0 (1.3)
K_2TcCl_6 [15]		257.7 (1.3)							285.0
K_2TcOCl_5 [15]		258.3(1.6)							285.0
$KTcO_4$ [15]		259.7(1.8)							285.0
Al_2O_3 [16]			74.8						
$AlPO_4$ [17]				133.9					284.8
α-Fe_2O_3 [16]					711.0				
Na_2O [16]						1072.5			
K_3PO_4 [16]				133.4			292.7	530.6	

Table 2. Dependence of the degree $N(Tc^{N+})$ of technetium oxidation on the binding energy E_b(Tc3d) of Tc3$d_{5/2}$-electrons. The spin-orbit splitting ΔE_{sl}(Tc3d) = 3.6 eV

$N(Tc^{N+})$	E_b(Tc3$d_{5/2}$)				
	a[a]	b[b]	c [24]	d [25]	e [26]
0	254.6	254.58	254.6	254.6	254.0
1	–	255.36	–	–	253.7
2	256.1	256.13	255.4	–	–
3	–	256.91	256.5	255.6	255.6
4	257.7	257.68	256.7	257.2	257.5
5	258.5	258.46	258.2	258.3	258.3
6	–	259.24	–	–	–
7	259.9	259.93	259.9	259.5	259.9

[a] The binding energies underlying Eq. (5) were obtained via reduction to the common scale (E_b(C1s) = 285.0 eV), and by analysis and averaging of the data from [24–26].
[b] Values furnished by Eq. (5).

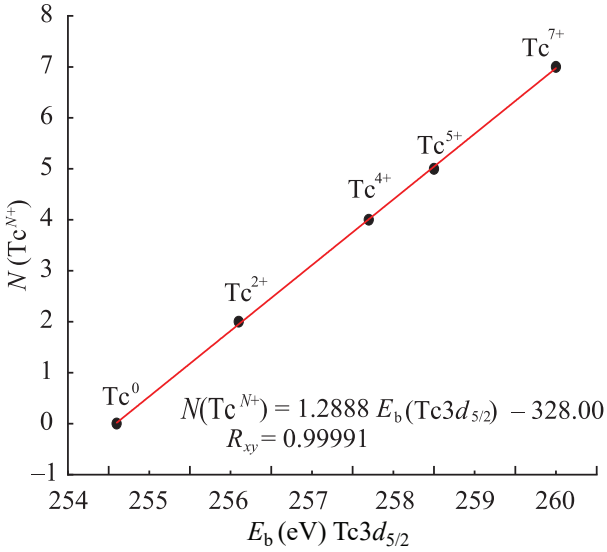

Fig. 4. Correlation between the degree $N(Tc^{N+})$ of technetium oxidation and the binding energy $E_b(Tc3d_{5/2})$ of $Tc3d_{5/2}$-electrons.

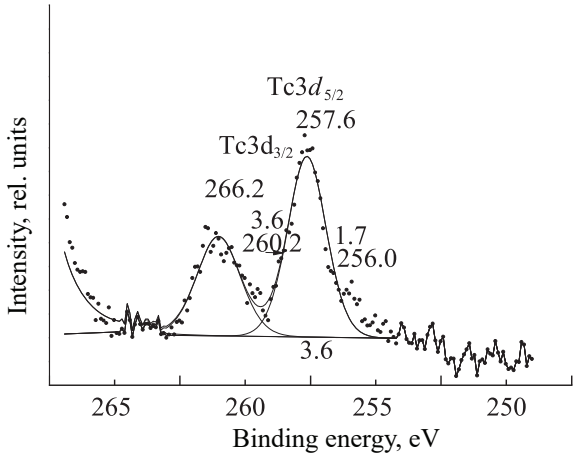

Fig. 5. XPS spectrum of Tc3*d*-electrons in a Tc-SAIP sample.

P–O–Fe bonds. The $R_{E–O}$ element-oxygen bond lengths (nm) were estimated with consideration for expression (4) from [22]:

$$R_{E–O}\ (nm) = 2.27(E_b - 519.4)^{-1}. \quad (4)$$

For the binding energies of O1*s*-electrons [531.2 and 532.6 eV (Table 1)], the bond lengths are, respectively, 0.186 and 0.169 nm. These values characterize the element–oxygen bond lengths on the surface of the samples studied. They are averaged over all lengths of bonds (P–O, Al–O, Fe-O, Na–O, Tc–O) present in a sample.

To obtain dependences of the degree of technetium oxidation $N(Tc^{N+})$ on the binding energy $E_b(Tc3d_{5/2})$ of $Tc3d_{5/2}$-electrons, the values of these energies for the known compounds of technetium [24–26] were reduced to the unified standard scale in which the binding energy of the aliphatic carbon of an adsorbed contaminant is $E_b(C1s) = 285.0$ eV [20]. For the values of $E_b(Tc3d_{5/2})$ for various degrees of technetium oxidation [24] were taken arithmetic means (Table 2, column *a*). These data served as a basis of a linear approximation to the dependence of the degree of technetium oxidation on the binding energy of $Tc3d_{5/2}$-electrons in accordance with Eq. (5)

$$N(Tc^{N+}) = 1.2888E_b(Tc3d_{5/2}) - 328.00, \quad (5)$$

where $R_{xy} = 0.99991$ is the Pearson's correlation coefficient (Fig. 4).

The binding energies obtained by using Eq. (5) for the degrees of oxidation in the range from 0 to 7 are listed in Table 2 (column *b*). The columns *c*, *d*, and *e* in Table 2 present for comparison the averaged published data on the binding energies of $Tc3d_{5/2}$ electrons for technetium compounds with various degrees of technetium oxidation.

Three doublets were observed for Tc3*d*-electrons in an XPS study of the products of the reaction with technetium [27] at 256.1, 258.0, and 259.9 eV. These doublets were attributed to Tc(IV), Tc(VI), and Tc(VII) ions, respectively. In accordance with Eq. (1), to these binding energies correspond the degrees of oxidation +1.96, +4.41, and +6.86. With consideration for the data in Table 2, to these degrees of oxidation correspond Tc(II),Tc(IV) ions or Tc(V) and Tc(VII). In this case, the gross error in determining the degree of oxidation is due to the calibration and identification of the spectrum. Therefore Eq. (1) can only be used to estimate the degree of oxidation of technetium ions.

To determine the degree of Tc oxidation, we used the lines of the doublet of Tc3*d*-electrons, related to the spin-orbital splitting with $\Delta E_{sl}/(Tc3d = 3.6$ eV (Fig. 5). The spectrum shows the main doublet at $\Delta E_b(Tc3d_{5/2}) =$ 257.6 eV. According to Eq. (2), the main doublet corresponds to the degree of technetium oxidation equal to 3.99. This suggests that mostly Tc(IV) ions are observed. It is known that Tc(VII) compounds are the most stable. However, in a high-temperature synthesis of a glass, technetium compounds may lose oxygen and be reduced to the state Tc(IV) [2].

It was found, on the basis of the intensities of lines of the XPS spectra of core electrons that the inclusion of Tc

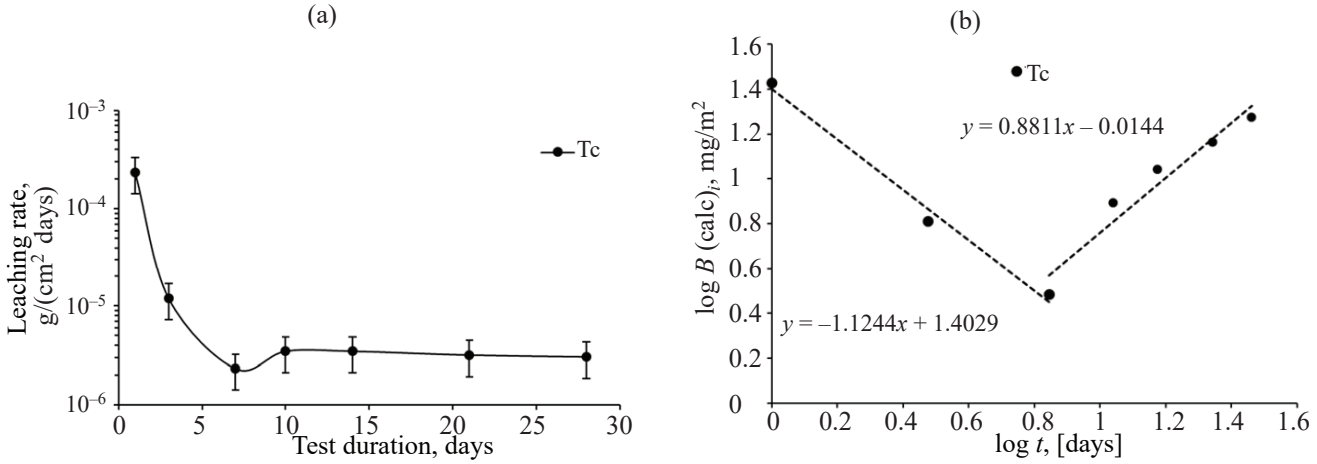

Fig. 6. (a) Differential rate of Tc leaching and (b) logarithmic dependence of the egress of Tc from a Tc-SAIP glass.

into the composition of the glass was not less than 60%. This is confirmed by the data obtained in determining the amount of technetium in trap solutions. It should also be noted that a decrease in the concentration of Na^+ ions is observed on the glass surface, whereas that of K^+ ions increases, which is due to their higher diffusion mobility [28].

Water resistance of the Tc-SAIP glass. The synthesized glass samples were subjected to leaching in accordance with the half-dynamic test of GOST R 52126–2003 [29]. The results obtained are presented in Fig. 6a. It was found that the rate of technetium leaching decreases in the course of the test (Fig. 6a) by 10th–28th day to values of about (2–4) × 10^{-6} g/(cm_2 day). This value is comparable with that for the rate of technetium leaching from a high-temperature borosilicate glass, the leaching rate from which is 1.1 × 10^{-6} g (m^2 day) by the 32nd day at a lower content of technetium in the starting glass (4.6 × 10^{-3} wt %) [30]. The high leaching rates during the first days of the test are characteristic of glass-like compounds, being due to the washing away from the glass surface [31].

To assess the mechanism of technetium leaching from the Tc-SAIP glass, we constructed a dependence in accordance with the model [18] (Fig. 6b). Previously, it has been shown [32–35] that to the values of the coefficients in Eq. (2) correspond the following element-leaching mechanisms: <0.35, washing away from the compound surface; 0.35–0.65, diffusion from inner layers; >0.65, dissolution of the surface layer of the compound. As a result, it was found, according to the data in Fig. 6b, that the leaching of technetium during the first 7 days occurs via washing away of technetium from the glass surface and, during the subsequent days, it corresponds to the mechanism of dissolution of the glass surface. It should be noted that, despite the already initiated dissolution process, the rate of technetium leaching remains lower than that from the borosilicate glass [2].

CONCLUSIONS

SAIP glass samples containing technetium in weight amounts were synthesized and studied. It was found that the degree of technetium oxidation is (IV). 83% of iron is present in the glass as Fe(III), and the rest, as Fe(II). The rate of Tc leaching from the glass at 90°C by 28th day is about 3 × 10^{-6} g/(cm^2 day) according to the half-dynamic test in conformity with GOST R 52126–2003, which is comparable with that from the borosilicate glass under these conditions. Thus, it was established that the use of the SAIP glass is promising for handling technetium-containing radioactive wastes.

FUNDING

The study was carried out under the State assignment for the Institute of Geochemistry and Analytical Chemistry, Russian Academy of Sciences (0137-2019-0022). The study used the equipment purchased by using the means of the Development Program of the M.V. Lomonosov State University in Moscow.

CONFLICT OF INTEREST

The authors state that they have no conflict of interest.

REFERENCES

1. Ogawa, T., *Fuels and Aterials for Transmutation,* OECD/NEA, NEA no. 5419, 2005.
2. Soderquist, Ch.Z., Schweiger, M.J., Kim, D.S.,

Lukens, W.W., and McCloy, J.S., *J. Nucl. Mater.,* 2014, vol. 449, p. 173.

3. Stefanovsky, S.V., Stefanovskaya, O.I., Vinokurov, S.E., Danilov, S.S., and Myasoedov, B.F., *Radiochemistry,* 2015, vol. 57, no. 4, p. 348. https://doi.org/10.1134/S1066362215040037
4. Danilov, S.S., Stefanovsky, S.V., Stefanovskaya, O.I., Vinokurov, S.E., Myasoedov, B.F., and Teterin, Yu.A., *Radiochemistry,* 2018, vol. 60, no. 4, p. 434. https://doi.org/10.1134/S1066362218040136
5. Stefanovsky, S.V., Maslakov, K.I., Teterin, Y.A., Kalmykov, S.N., Danilov, S.S., Teterin, A.Y., and Ivanov, K.E., *Dokl. Phys. Chem.,* 2018, vol. 47, no. 1, p. 6.
6. Stefanovskii, S.V., Stefanovskaya, O.I., Semenova, D.V., Kadyko, M.I., and Danilov, S.S., *Glass Ceram.,* 2018, vol. 75, nos. 3–4, p. 89.
7. Stefanovsky, S.V., Sefanovsky, O.I., Myasoedov, B.F, Vinokurov, S.E., Danilov, S.S., Nikonov, B.S., Maslakov, K.I., and Teterin, Yu.A., *J. Non-Cryst. Solids,* 2017, vol. 471, p. 421.
8. Maslakov, K.I., Teterin, Yu.A., Stefanovsky, S.V., Kalmykov S.N., Teterin A.Yu., Ivanov, K.E., and Danilov, S.S., *J. Non-Cryst. Solids,* 2018, vol. 482, p. 23.
9. Danilov, S.S., Frolova, A.V., Kulikova, S.A., Vinokurov, S.E., Maslakov, K.I., Teterin, Yu.A., Teterin, A.Yu., Myasoedov, B.F., *Radiochemistry*, 2021, vol. 63, no. 1, p. 99.

   https://doi.org/10.1134/S106636222101015X
10. Rabinovich, V.A. and Khavin, Z.Ya., *Kratkii khimicheskii spravochnik* (Brief Chemical Handbook), Potekhina, A.A. and Efimova, A.I., Eds., Leningrad: Khimiya, 1991.
11. Lukens, W.W., McKeown, D.A., Buechele, A.C., Muller, I.S., Shuh, D.K., and Pegg, I.L., *Chem. Mater.,* 2007, vol. 19, no. 3, p. 559.
12. Muller, I.S., Viragh, C., Gan, H., Matlack, K.S., and Pegg, I.L., *Hyperfine Interact.,* 2009, vol. 191, no. 1, p. 17.
13. Bekman, I.N., *Neorganicheskaya khimiya. Radioaktivnye elementy: uchebnik dlya bakalavriata i magistratury* (Inorganic Chemistry. Radioactive Elements: Textbook for Undergraduate and Graduate Programs), Moscow: Yurait, 2017.
14. Stefanovsky, S.V., Prusakov, I.L., Stefanovsky, O.I., Kadyko, M.I., Averin, A.A., Makarenkov, V.I., Trigub, A.I., and Nikonov, B.S., *Int. J. Appl. Glass Sci.,* 2019, vol. 10, no. 4, p. 479.
15. Shirley, D.A., *Phys. Rev. B,* 1972, vol. 5, no. 12, p. 4709.
16. Nemoshkalenko, V.V. and Aleshin, V.G., *Elektronnaya spektroskopiya kristallov* (Electronic Spectroscopy of Crystals), Kiev: Nauk. dumka, 1976.
17. Scofield, J.H., *J. Electron Spectrosc. Relat. Phenom.*, 1976, vol. 8, no. 2, p. 129.
18. De Groot, G.J. and Van der Sloot, H.A., *Stabilization and Solidification of Hazardous, Radioactive and Mixed Wastes,* Gilliam, T.M., and Wiles, C.C., Eds., Philadelphia: ASTM, 1992, vol. 2, p. 149.
19. Maslakov, K.I., Teterin Yu.A., Stefanovsky, S., Kalmykov St.N., Teterin A.Yu., Ivanov, K.E., J. Alloys Compd., 2017, vol. 712, p. 36.
20. Nefedov, V.I., *Rentgenoelektronnaya spektroskopiya khimicheskikh soedinenii* (X-ray Electron Spectroscopy of Chemical Compounds), Moscow: Khimiya, 1984.
21. Yamashita, T. and Hayes, P., *Appl. Surf. Sci.,* 2008, vol. 254, no. 8, p. 2441.
22. Sosulnikov, M.I. and Teterin, Y.A., *J. Electron Spectrosc. Relat. Phenom.*, 1992, vol. 59, no. 2, p. 111.
23. Lindblad, T., Rebenstorf, B., Yan Z.-G., and Andersson, S.L.T., *Appl. Catal. A: General,* 1994, vol. 112, no. 2, p. 187.
24. Gerasimov, V.N., Kuzina, A.F., Kulakov, V.M., Kryuchkov, C.B., Abstracts of Papers, *IV seminara spetsialistov sots. stran po elektronnoi spektroskopii, Moscow, 2–16 maya 1982 g* (IV Workshop of Specialists from Socialist Countries on Electron Spectroscopy, Moscow, May 2–16, 1982), Moscow: Inst. Obshch. Neorg. Khim. Akad. Nauk SSSR, 1982.
25. Thompson, M., Nunn A.D., and Treher, E.N., *Anal. Chem.,* 1986, vol. 58, no. 14, p. 3100.
26. Wester, D.W., White, D.H., Miller, F.W., Dean, R.T., Schreifels, J.A., and Hunt, J.E., *Inorg. Chim. Acta,* 1987, vol. 131, no. 2, p. 163.
27. Chatterjee, S., Hall, G.B, Johnson, I.E., Du, Y., Walter, E.D., Washton, N.M., and Levitskaia, T.G., *Inorg. Chem. Front.,* 2018, vol. 5, no. 9, p. 2081.
28. Frischat, G.H., *Ionic Diffusion in Oxide Glasses,* Ohio: Trans Tech, 1975.
29. GOST R (State Standard R) 52126-2003: Radioactive Waste. Determination of the Chemical Stability of Solidified High-Level Waste by the Long-Term Leaching Method, Moscow: Gosstandart Rossii, 2003.
30. Bradley, D.J., Harvey, C.O., and Turcotte, R.P., *Battelle Pacific Northwest Labs.,* 1979, no. PNL-3152.
31. Vlasova, N.V., Remizov, M.B., Kozlov, P.V., and Belanova, E.A., *Vopr. Radiats. Bezop.,* 2017, no. 3, p. 32.
32. Vinokurov, S.E., Kulikova, S.A., Krupskaya, V.V., and Myasoedov, B.F., *Radiochemistry,* 2018, vol. 60, no. 1, p. 70. https://doi.org/10.1134/S1066362218010125
33. Vinokurov, S.E., Kulikova, S.A., Belova, K.Yu., Rodionova, A.A., and Myasoedov, B.F., *Radiochemistry,* 2018, vol. 60, no. 6, p. 644. https://doi.org/10.1134/S1066362218060139
34. Vinokurov, S.E., Kulikova, S.A., and Myasoedov, B.F., *J. Radioanal. Nucl. Chem.,* 2018, vol. 318, no. 3, p. 2401.
35. Xue, Q., Wang, P., Li, J.-S., Zhang, T.-T., and Wang, S.-Y., *Chemosphere,* 2017, vol. 166, p. 1.